Int. J. Fuzzy Syst. (2021) 23(7):1919–1933
https://doi.org/10.1007/s40815-021-01097-8

Evaluating Power Rehabilitation Actions Using a Fuzzy Inference Method

Yo-Ping Huang[1,2,3] · Wen-Lin Kuo[1] · Haobijam Basanta[1] · Si-Huei Lee[4,5]

Received: 26 December 2020 / Revised: 26 December 2020 / Accepted: 1 April 2021 / Published online: 20 June 2021

Abstract The older population faces a high probability of experiencing age-related problems, such as osteoporosis, immobility, gait disturbances, stroke, Parkinson's disease, and cognitive behavioral functional difficulties. Such problems negatively affect their lives. Thus, access to long-term care is a critical issue for older adults. In response to the aforementioned serious health issues, society must strive to provide a supportive and effective rehabilitation environment for older adults. This study designed an intelligent active and passive limb rehabilitation system to track and quantify the effectiveness of joint movements in patients automatically. The proposed method uses a camera and PoseNet to capture key feature information regarding human skeleton nodes and identify rehabilitation actions through joint movements. In addition, to solve the problem of joint occlusion during joint angle measurement, the designed system is equipped with a self-designed inertial measurement unit with GY-85 nine-axis sensors, which are mounted on the occluding part of the joints. A fuzzy inference system was developed to provide scores, suggestions, and encouragement for each rehabilitation session. This system also provides an interactive interface for users to monitor each rehabilitation session and examine whether rehabilitation is performed accurately.

Keywords Power rehabilitation · Fuzzy inference system · Parkinson's disease · Inertial measurement unit (IMU)

✉ Yo-Ping Huang
yphuang@ntut.edu.tw

✉ Si-Huei Lee
leesihuei@gmail.com

Wen-Lin Kuo
kitecycling@gmail.com

Haobijam Basanta
basantameitei@gmail.com

[1] Department of Electrical Engineering, National Taipei University of Technology, Taipei 10608, Taiwan

[2] Department of Computer Science and Information Engineering, National Taipei University, New Taipei City 23741, Taiwan

[3] Department of Information and Communication Engineering, Chaoyang University of Technology, Taichung 41349, Taiwan

[4] Department of Physical Medicine and Rehabilitation, Taipei Veterans General Hospital, Taipei 11217, Taiwan

[5] Department of Medicine, National Yang Ming University, Taipei 11221, Taiwan

1 Introduction

In developed countries, the population of those aged 60 years or older is growing faster than the populations of other age groups. A survey of world population prospects conducted in 2019 projected that 1 in 6 people in the world (16% of the global population) would be older than 65 years by 2050. By comparison, in 2019, 1 in 11 people in the world (9% of the global population) were older than 65 years [1]. This projected demographic shift will pose significant challenges for health care systems and increase the demand for long-term care. Age-associated conditions cause multimorbidity and geriatric syndromes [2], such as frailty [3], delirium [4], impaired cognition [5], visual impairment, and sarcopenia [6], among aging populations [7, 8]. The aforementioned conditions increase the risk of disability with impairments in activities of daily living. Parkinson's disease (PD), dementia, and stroke [9] are major and common chronic diseases faced by the elderly

that are associated with impaired mobility, tremor, limb stiffness, decreased motor function, and abnormal gait. The clinical assessment of older people with disability and impairments in body functioning is challenging. Nearly two-thirds of people admitted to hospitals are over 65 years old [10] and have been diagnosed with PD or dementia [11]. In the case of acute illnesses, individuals older than 65 years face a significantly longer length of hospital stay than those younger than 65 years do. In the case of older individuals with acute illnesses, rehabilitation is considered the most important factor for regaining and maintaining optimal physical functioning in daily life [12]. Rehabilitation exercises usually involve different joint kinematics, including flexion, extension, abduction, rotation, and deviation of body function [13]. Thus, rehabilitation exercises focus on the posture during an action and joint movement ability of an individual [14].

Although evidence exists regarding the clinical effectiveness of rehabilitation services, inadequate rehabilitation services are available to many elderly people [15]. The reasons for this phenomenon include the high number of patients with multiple long-term conditions who require rehabilitation services; the complex set of processes involved in these services, which usually requires several professional practitioners across the entire continuum of rehabilitation to conduct monitoring and provide assistance; and the lack of comprehensive organization of care for evaluating therapeutic interventions according to the patient's clinical context and needs. To provide a holistic assessment of rehabilitation, we designed a rehabilitation system that includes wearable sensors to calculate the joint angles of patients. An embedded camera is used to capture the performance of different therapies precisely on the basis of key feature information regarding a patient's posture. To address the limited availability of experts and physical therapists, an interactive interface is incorporated into the system to enable users to monitor each rehabilitation session and ensure that the rehabilitation exercises are performed correctly. Furthermore, to determine the effectiveness of rehabilitation, the signals transmitted by the rehabilitation devices are stored on a cloud; thus, patients who require regular rehabilitation at home can be assisted and monitored by practitioners and provided information on the progress of their rehabilitation instantly.

Major contributions of this study include:

- a fuzzy inference model is proposed to objectively score the rehabilitation exercises based on sensor readings;
- multiperson rehabilitation at the same time is allowed;
- multifactorial rehabilitation can deal with joints movement, range of motion, and posture are possible;
- alert of wrong joint exercise with flash light is provided;
- individual guide videos on the reference exercise are played for each participant;
- a patient can self-rehabilitate at home that greatly reduces the manpower needs of the rehabilitation.

The remainder of this paper is organized as follows: Sect. 2 presents the background of the fuzzy inference models required in the study. Section 3 describes the design methodology for the proposed rehabilitation system. Section 4 provides the experimental results. Section 5 presents a discussion of the research results and a comparison of these results with those of related studies. Finally, Sect. 6 presents the conclusions of this study and recommendation for future studies.

2 Background of the Present Study

This section provides an overview of fuzzy applications to address the uncertainty of event scores obtained during rehabilitation exercises. PoseNet is used to obtain key features of the human anatomy, and the direction cosine matrix (DCM) is used to determine the rotations of wearable sensors in different coordinate systems.

2.1 Fuzzy Implication of Uncertain Rehabilitation Events

Rehabilitation exercises usually involve different joint arthrokinematics, including flexion, extension, abduction, adduction, medial and lateral rotation, and deviation [16–18], to increase the mobility of restricted joints or muscles and gradually restoring the stability of motion. The mechanistic modeling of physical therapy is often complicated by the presence of uncertainties. Moreover, the functional abilities of muscular strength and endurance are assessed using subjective estimation or expert personal experiences and classical logic [such as pass (1) or fail (0)]. The modeling of real situations with a conventional decision model may not indicate the degree to which a decision is certain and reliable for joint muscular strength and endurance, range of motion, or significant increases in the customizable parameters of every individual rehabilitation, for example.

Suppose that a patient must execute a chest press during rehabilitation. A chest press involves left and right shoulder abduction as well as left and right elbow flexion. A physical therapist stands near the patient to evaluate the patient's performance visually on the basis of a preset baseline. By referring to the baseline, the physical therapist marks an abduction as either "passed" or "failed" on the

patient's score sheet. No partial score can be provided even if the extent of abduction was marginally below the baseline. In this situation, the evaluation considerably depends on the visual judgment of the physical therapist, not a quantitative approach that may not be applicable to real-time scenarios. In contrast to the aforementioned method, a fuzzy-logic-based approach enables the consideration of uncertainties associated with a decision [19, 20].

The possible distribution of a sensor's readings can be represented by its corresponding degree of membership using a predefined fuzzy set. For instance, suppose that $U = \{\mathrm{re}_1, \mathrm{re}_2,\ldots,\mathrm{re}_i,\ldots,\mathrm{re}_n\}$, $i = 1, 2,\ldots,n$, represents a universal set for n rehabilitation events. In this case, the individual sensor readings obtained during a sequence of exercises can be characterized by linguistic variables such as low, moderate, high, and full. To indicate changes in sensor readings, we can define a fuzzy set X based on the rehabilitation event as follows:

$$X = \frac{\mu(\mathrm{re}_1)}{\mathrm{re}_1} + \frac{\mu(\mathrm{re}_2)}{\mathrm{re}_2} + \cdots \frac{\mu(\mathrm{re}_i)}{\mathrm{re}_i} + \cdots + \frac{\mu(\mathrm{re}_n)}{\mathrm{re}_{n1}}, \tag{1}$$

where $\mu(\mathrm{re}_i)$ represents a membership degree between [0, 1] for the rehabilitation event re_i associated with the fuzzy set X.

2.2 Fuzzy Inference System

A fuzzy inference system, FIS [21] is used to map input patterns to infer their desired output. The number of fuzzy rules can be selected manually by the user or automatically generated from the combinations of labels assigned for the input variables. The implementation of the FIS involves the following steps:

- Step 1 Each input and output variable and a set of its corresponding membership functions is defined in advance. Furthermore, a fuzzy rule base that correlates the input and output variables is also generated.
- Step 2 Input data are fuzzified using membership functions.
- Step 3 The t-norm operation is applied to the antecedent part of the rule to calculate the firing strength of a rule.
- Step 4 A set of sensor readings may activate more than one rule simultaneously. A decision-making logic based on the t-conorm operation is used for determining the fuzzy output.
- Step 5 A defuzzification process is used to infer a crisp output value.

2.3 Direction Cosine Matrix

A DCM, which is also referred to as a rotation matrix, defines the rotation of one coordinate frame with respect to another coordinate frame. It uses three-dimensional Cartesian coordinates to represent the global coordinate system and the body coordinate system of an object (i.e., O_{XYZ} and O_{xyz}, respectively). In Fig. 1, X, **Y**, **Z**, **R**, **x**, **y**, and **z** are unit vectors. Both the global and local coordinate systems have a fixed origin, namely O (Fig. 1). The DCM representing the attitude of the body can be converted by rotating the reference coordinate system specified by a 3×3 matrix; thus, any vector in the body coordinate system O_{xyz} can be converted into a vector in the global coordinate system O_{XYZ} using a rotation matrix.

A vector **x** in the body coordinate system O_{xyz} can be represented in the global coordinate system O_{XYZ} as follows:

$$x^{\mathrm{G}} = \left[x_x{}^{\mathrm{G}}, x_y{}^{\mathrm{G}}, x_z{}^{\mathrm{G}}\right]^{\mathrm{T}}, \tag{2}$$

where $\mathbf{x}^{\mathbf{G}}$ is the converted vector represented in the global coordinate system and $[\ldots]^{\mathrm{T}}$ is a column vector that has been transposed to a row vector. Thus, $\mathbf{x}_{\mathbf{x}}{}^{\mathbf{G}}$ can be expressed as follows: $\mathbf{x}_{\mathbf{x}}{}^{\mathbf{G}} = |X||x|\cos(X,x) = X \cdot x$, where $|x|$ is the magnitude of the unit vector and $\cos(X,x)$ is the cosine of the angle between vectors **X** and **x**. The inner product of **X** and **x** is expressed as $X \cdot x$. Thus, $\mathbf{x}^{\mathbf{G}}$, $\mathbf{y}^{\mathbf{G}}$, and $\mathbf{z}^{\mathbf{G}}$ can be rewritten as follows:

$$x^{\mathrm{G}} = [X \cdot x, Y \cdot x, Z \cdot x]^{\mathrm{T}}, \tag{3}$$

$$y^{\mathrm{G}} = [X \cdot y, Y \cdot y, Z \cdot y]^{\mathrm{T}}, \tag{4}$$

$$z^{\mathrm{G}} = [X \cdot z, Y \cdot z, Z \cdot z]^{\mathrm{T}}, \tag{5}$$

$$\begin{aligned}\left[x^{\mathrm{G}}, y^{\mathrm{G}}, z^{\mathrm{G}}\right] &= \begin{bmatrix} X \cdot x & X \cdot y & X \cdot z \\ Y \cdot x & Y \cdot y & Y \cdot z \\ Z \cdot x & Z \cdot y & Z \cdot z \end{bmatrix} \\ &= \begin{bmatrix} \cos(X,x) & \cos(X,y) & \cos(X,z) \\ \cos(Y,x) & \cos(Y,y) & \cos(Y,z) \\ \cos(Z,x) & \cos(Z,y) & \cos(Z,z) \end{bmatrix} \\ &= \mathrm{DCM}^{\mathrm{G}}. \end{aligned} \tag{6}$$

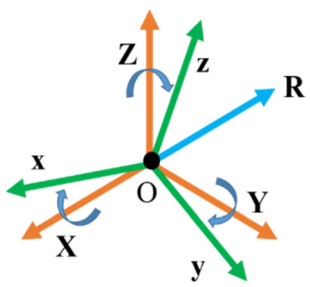

Fig. 1 Coordinates of the DCM

Similarly, a vector in the global coordinate system O_{XYZ} can be converted into the body coordinate system O_{xyz} as follows:

$$\begin{aligned}\left[X^{\mathrm{L}}, Y^{\mathrm{L}}, Z^{\mathrm{L}}\right] &= \begin{bmatrix} X\cdot x & Y\cdot x & Z\cdot x \\ X\cdot y & Y\cdot y & Z\cdot y \\ X\cdot z & Y\cdot z & Z\cdot z \end{bmatrix} \\ &= \begin{bmatrix} \cos(X,x) & \cos(Y,x) & \cos(Z,x) \\ \cos(X,y) & \cos(Y,y) & \cos(Z,y) \\ \cos(X,z) & \cos(Y,z) & \cos(Z,z) \end{bmatrix} \\ &= \mathrm{DCM}^{\mathrm{L}}. \end{aligned} \tag{7}$$

The DCM is used for orienting a rigid body at a desired attitude. Thus, it can also be used to determine the global coordinates of an arbitrary vector if the coordinates of this vector in the body coordinate frame are known. For instance, if a vector in the body coordinate system O_{xyz} can be represented as $\mathbf{r}^{\mathbf{L}} = \left[{r_x}^{\mathrm{L}}, {r_y}^{\mathrm{L}}, {r_z}^{\mathrm{L}}\right]^{\mathrm{T}}$, its coordinates in the global coordinate system O_{XYZ} can be expressed as $\mathbf{r}^{\mathbf{G}} = \left[{r_x}^{\mathrm{G}}, {r_y}^{\mathrm{G}}, {r_z}^{\mathrm{G}}\right]^{\mathrm{T}}$ using a known rotation matrix, namely $\mathbf{DCM}^{\mathbf{G}}$; thus, $\left|r^{\mathrm{G}}\right| = |r^{\mathrm{L}}| = 1$ and $\cos\left(X^{\mathrm{G}}, r^{\mathrm{G}}\right) = \cos\left(X^{\mathrm{L}}, r^{\mathrm{L}}\right)$. Consequently, the following expression is obtained:

$${r_x}^{\mathrm{G}} = \left|r^{\mathrm{G}}\right|\cos\left(X^{\mathrm{G}}, r^{\mathrm{G}}\right) = X^{\mathrm{L}}\cdot r^{\mathrm{L}}. \tag{8}$$

By substituting the expression $\mathbf{X}^{\mathbf{L}} = [X\cdot x, X\cdot y, X\cdot z]^{\mathrm{T}}$ in Eq. (8), the following equation is obtained:

$${r_x}^{\mathrm{G}} = {r_x}^{\mathrm{L}} X\cdot x + {r_y}^{\mathrm{L}} X\cdot y + {r_z}^{\mathrm{L}} X\cdot z. \tag{9}$$

Finally, the rotation matrix for conversion from the body coordinate system to the global coordinate system can be expressed as follows:

$$r^{\mathrm{G}} = \begin{bmatrix} {r_x}^{\mathrm{G}} \\ {r_y}^{\mathrm{G}} \\ {r_z}^{\mathrm{G}} \end{bmatrix} = \begin{bmatrix} X\cdot x & X\cdot y & X\cdot z \\ Y\cdot x & Y\cdot y & Y\cdot z \\ Z\cdot x & Z\cdot y & Z\cdot z \end{bmatrix} \begin{bmatrix} {r_x}^{\mathrm{L}} \\ {r_y}^{\mathrm{L}} \\ {r_z}^{\mathrm{L}} \end{bmatrix} = \mathrm{DCM}^{\mathrm{G}} r^{\mathrm{L}}. \tag{10}$$

2.4 Euler Angles

The transformation of a rigid body to a desired attitude can be achieved by conducting successive rotations along the X-, Y-, and Z-axes. In terms of the Euler angle, the aforementioned rotation can be represented as successive rotations along the z-, y-, and x-axes. The angle of rotation about the y-axis is called the pitch angle (θ); that around the x-axis is called the roll angle (φ); and that around the z-axis is called the yaw angle (ψ). The relationships of the DCM with θ, φ, and ψ can be expressed as follows:

$$\mathrm{DCM}^{\mathrm{G}} = R(\psi,\theta,\varphi) = R_z(\psi)R_y(\theta)R_x(\varphi), \tag{11}$$

$$R_z(\psi) = \begin{bmatrix} \cos\psi & -\sin\psi & 0 \\ \sin\psi & \cos\psi & 0 \\ 0 & 0 & 1 \end{bmatrix}, \tag{12}$$

$$R_y(\theta) = \begin{bmatrix} \cos\theta & 0 & \sin\theta \\ 0 & 1 & 0 \\ -\sin\theta & 0 & \cos\theta \end{bmatrix}, \tag{13}$$

$$R_x(\varphi) = \begin{bmatrix} 1 & 0 & 0 \\ 0 & \cos\varphi & -\sin\varphi \\ 0 & \sin\varphi & \cos\varphi \end{bmatrix}. \tag{14}$$

Thus, a rotation R about any arbitrary axis is expressed in terms of successive rotations about the Z-, Y-, and X-axes by performing matrix multiplication as follows:

$$R = \begin{bmatrix} \cos\theta\cos\psi & \sin\varphi\sin\theta\cos\psi - \cos\varphi\sin\psi & \cos\varphi\sin\theta\cos\psi + \sin\varphi\sin\psi \\ \cos\theta\sin\psi & \sin\varphi\sin\theta\sin\psi + \cos\varphi\cos\psi & \cos\varphi\sin\theta\sin\psi - \sin\varphi\cos\psi \\ -\sin\theta & \sin\varphi\cos\theta & \cos\varphi\cos\theta \end{bmatrix}. \tag{15}$$

2.5 Pose Estimator

Pose estimation using a webcam has transformed many healthcare applications by enabling the tracking of a patient's joints and posture. The captured stances provide quantitative data that can be experimentally and clinically informative. A pose estimation system can streamline the data analytics process for patient progress in real time. After experimentation with multiple computer vision techniques for pose estimation, we selected OpenPose [22] for pose detection. OpenPose is a deep learning algorithm that processes images through a two-branch multistage convolutional neural network. The first branch predicts the possible localization of human joints in an image according to the confidence score. The second branch implements partial affinity fields to predict a set of two-dimensional vectors that encodes the degree of association between the position and orientation of limbs over the image domain. The output of OpenPose consists of confidence maps and partial affinity fields that are parsed through greedy inference to associate body parts with individuals in an image. To localize a set of coordinates connected to human joints, 17 key points of the human pose, including the nose, neck, shoulders, elbows, wrists, hips, knees, and ankles, are considered.

3 Design and Methodology

In this section, we describe the architecture of the proposed system as well as the design of processes and functions to make rehabilitation for older patients more preventative and accessible.

3.1 Hardware Design

The proposed rehabilitation monitoring and evaluation system contains hardware devices such as a webcam, Arduino microcontrollers, an ADXL345 accelerometer, an ITG3205 gyroscope, an HMC5883L magnetometer, a CD74HC4067 multiplexer, and two HC-05 Bluetooth wireless transmission modules. Figure 2 shows the hardware architecture of the proposed rehabilitation monitoring and evaluation system, which comprises 10 nine-axis sensors, 12 Arduino Nano microcontrollers, an Arduino Mega 2560 microcontroller, two 16-channel analog MUX modules, a pair of HC-05 Bluetooth transmission modules, and a USB-to-TTL conversion module. Figure 3 displays the physical setup of the sensing devices that are mounted on the joints of the rehabilitation patients. Figure 4 depicts the circuit configuration of the nine-axis sensing device.

3.2 Application of the Nine-Axis Sensors According to the DCM

This section describes how to read the values of the nine-axis sensors, three-axis gyroscope, three-axis accelerometer, and three-axis magnetometer. Gyroscopes are unable to indicate the absolute device orientation, whereas accelerometers and magnetometers provide the most accurate estimation of the device orientation. The readings obtained from the accelerometer, magnetometer, and gyroscope are adopted in a fusion algorithm developed in this study.

A DCM that contains a vector of the global coordinate system in each row can be defined as follows:

$$\mathbf{DCM^G} = \left[\mathbf{x^G}, \mathbf{y^G}, \mathbf{z^G}\right] = \begin{bmatrix} \mathbf{X^{BT}} \\ \mathbf{Y^{BT}} \\ \mathbf{Z^{BT}} \end{bmatrix}, \tag{16}$$

where $\mathbf{DCM^G}$ is the global DCM; $\mathbf{x^G}, \mathbf{y^G}$, and$\mathbf{z^G}$ are global unit vectors; and $\mathbf{X^{BT}}$, $\mathbf{Y^{BT}}$, and $\mathbf{Z^{BT}}$ are the vectors in the

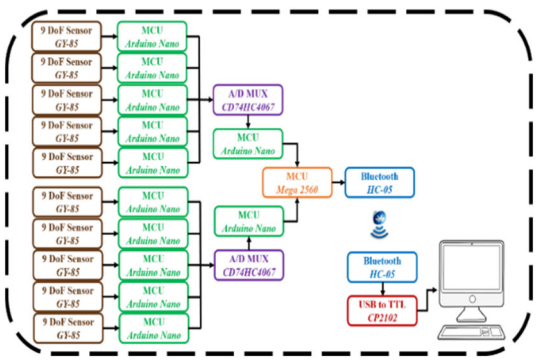

Fig. 2 Hardware architecture of the proposed rehabilitation monitoring and evaluation system

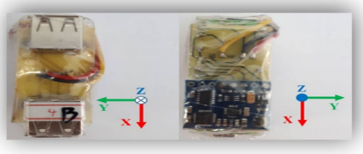

Fig. 3 Physical setup of the nine-axis sensing device

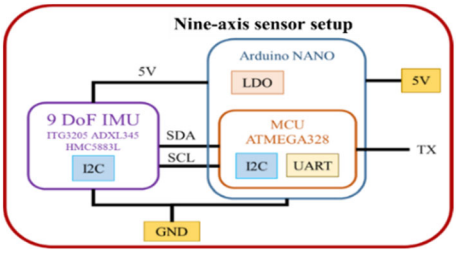

Fig. 4 Circuit configuration of the nine-axis sensing devices

body coordinate system. On the basis of Eq. (16), let the accelerometer reading be Z^{BT}, with the starting point at time t_0; then, the acceleration value is Z_0^{B} and the gyroscope value is ω_0. The acceleration value at the subsequent moment (Z_1^{B}) is estimated from the gyroscope value as follows:

$$Z_1^{\mathrm{B}} \approx Z_0^{\mathrm{B}} + \mathrm{d}tV = Z_0^{\mathrm{B}} + \mathrm{d}t\left(\omega_0 \times Z_0^{\mathrm{B}}\right) = Z_0^{\mathrm{B}} + \left(\mathrm{d}\theta_{\mathrm{g}} \times Z_0^{\mathrm{B}}\right). \tag{17}$$

The reading obtained from the accelerometer is directly expressed as $Z_{1\mathrm{A}}^{\mathrm{B}}$, and the angular displacement and angular velocity of the gyroscope can be obtained from the acceleration reading as follows:

$$\mathrm{d}\theta_{\mathrm{a}} = \mathrm{d}t\omega_{\mathrm{a}}, \tag{18}$$

$$\omega_{\mathrm{a}} = Z_0^{\mathrm{B}} \times V_{\mathrm{a}} / \left|Z_0^{\mathrm{B}}\right|^2, \tag{19}$$

where ω_{a} is the angular velocity measured by the gyroscope, $\mathrm{d}\theta_{\mathrm{a}}$ is the angular displacement, and V_{a} is the linear velocity. Then, the following equation is obtained:

$$V_{\mathrm{a}} = \left(Z_{1\mathrm{A}}^{\mathrm{B}} - Z_0^{\mathrm{B}}\right)/\mathrm{d}t. \tag{20}$$

Equation (20) basically expresses the linear velocity of the vector $\mathbf{Z_0^B}$. Because $\mathbf{Z_0^B}$ is a unit vector, it can be expressed as follows:

$$\mathrm{d}\theta_{\mathrm{a}} = Z_0^{\mathrm{B}} \times \left(Z_{1\mathrm{A}}^{\mathrm{B}} - Z_0^{\mathrm{B}}\right), \tag{21}$$

where $Z_{1\mathrm{A}}^{\mathrm{B}}$ is the new accelerometer reading.

The aim of calculating a new estimate ($Z_{1\mathrm{A}}^{\mathrm{B}}$) is to obtain $\mathrm{d}\theta$ as a weighted average of $\mathrm{d}\theta_{\mathrm{a}}$ and $\mathrm{d}\theta_{\mathrm{g}}$. Because the magnetometer parameters are not used in the aforementioned operation, a significant drift occurs in the rotation angle ψ. The operation of the magnetometer is similar to

that for the accelerometer. The only difference is that the Z-axis is changed to the X-axis, that is, the vector pointing north is estimated. However, the sensor readings do not necessarily result in the Z- and X-axis being orthogonal to each other every time. Consequently, error accumulation occurs and the represented body is no longer a rigid body. Thus, the errors must be corrected.

The DCM is renormalized to obtain an orthogonal relationship between the X- and Z-axes. For instance, allocating errors for Z and X rows and rotating them in opposite direction by cross coupling defined as:

$$Z_{\text{orthogonal}} = Z - \frac{\text{error}}{2} X, \tag{22}$$

$$X_{\text{orthogonal}} = X - \frac{\text{error}}{2} Z. \tag{23}$$

The Y row of the matrix was adjusted to be orthogonal to the Z and X rows. The cross product of the corrected Z and X rows is expressed as follows:

$$Y_{\text{orthogonal}} = Z_{\text{orthogonal}} \times X_{\text{orthogonal}}. \tag{24}$$

Finally, the three-axis vector is normalized as follows:

$$X_{\text{orthogonal\_}} = \frac{1}{2}\left(3 - X_{\text{orthogonal}} \bullet X_{\text{orthogonal}}\right) X_{\text{orthogonal}}, \tag{25}$$

$$Y_{\text{orthogonal\_}} = \frac{1}{2}\left(3 - Y_{\text{orthogonal}} \bullet Y_{\text{orthogonal}}\right) Y_{\text{orthogonal}}, \tag{26}$$

$$Z_{\text{orthogonal\_}} = \frac{1}{2}\left(3 - Z_{\text{orthogonal}} \bullet Z_{\text{orthogonal}}\right) Z_{\text{orthogonal}}. \tag{27}$$

In this manner, the readings obtained from the accelerometer, gyroscope, and magnetometer can be combined to construct the DCM.

3.3 Execution of the Proposed Rehabilitation System

The proposed system mainly includes two modules. The first module includes a network camera for capturing the key features of anatomical joints, from which the joint angles are calculated. The obtained information is stored on a computer. In the second module, to avoid the occlusion of joint angles during rehabilitation, 10 sensing units are worn on 10 joints of the body, such as in both forearms, the upper arms of both hands, the T1 and S2 positions of the spine, the thighs, and the calves. A Unity 3D model running on the computer is used to simulate the joint angle signals of patients, as illustrated in Fig. 5.

The joint angle signals of patients are calculated from the data of sensors such as accelerometers and magnetometers using the DCM algorithm based on the Euler angles of pitch, roll, and yaw to evaluate the ability of anatomical joints and limbs. The calculated signals are stored on a cloud server to enable therapists and other practitioners to track and assist the rehabilitation of patients.

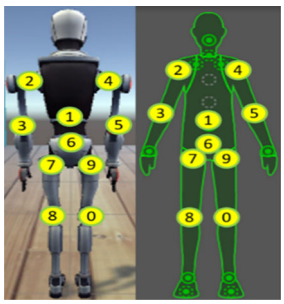

Fig. 5 Sensor-wearing positions corresponding to the joint points of the character model

3.4 Interactive Interface for Rehabilitation

The main interface for personal rehabilitation is depicted in Fig. 6. During exercise, this interface provides functions such as character model calibration, exercise selection, guide video display, motion correction prompts, and feature angle recording. After the sensors are mounted and the rehabilitation module is set up, the movement of the character model is simulated in a mirrored manner. For example, if the patient moves their left foot, the character model moves its right foot. If the joint and limb movements are incorrect, a yellow flashing light is triggered on the calibrated model to prompt the patient to appropriately correct their performance of the rehabilitation exercise.

The proposed system permits multiperson rehabilitation. During multiperson rehabilitation, individual guide videos on the reference exercise are played for each participant. To track the individual abilities of joints and sensor readings efficiently, the system setup for all individuals is uniformly operated using the main console interface.

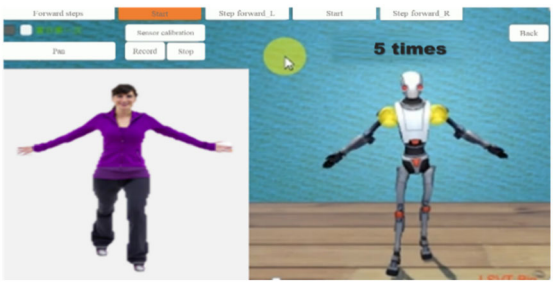

Fig. 6 Interactive interface for personal rehabilitation

4 Experimental Results

4.1 Demographic Data

An experiment was conducted with eight healthy participants. The statistical data of the participants are presented as means ± standard deviations in Table 1. The participants were aged 22–25 years, and their mean age was 23.63 ± 1.06 years. Their weights were between 50 and 73 kg, and their mean weight was 65.88 ± 7.95 kg. The heights of the participants were between 160 and 178 cm, and their mean height was 170.63 ± 6.25 cm.

4.2 Rehabilitation Exercise and Fuzzy Rules

To obtain quantitative and qualitative results for joint movements, four joint movement exercises were conducted: (a) the chest press, (b) the seated row, (c) torso flexion, and (d) leg extension. In each rehabilitation exercise, the participants were divided into groups of two people and their joint angles were recorded. Table 2 presents a detailed description of the rehabilitation exercises, and Fig. 7 illustrates the graphical posture of the exercises.

Figure 8 shows the proposed FIS for the sensor data. In this system, the joint inputs are transformed into degrees of membership by projecting the input numerical values into a set of membership functions with predefined fuzzy sets. The membership functions of joint angle difference are defined as follows: 0°–25°, zero; 10°–35°, small; and 25°–50°, large. The membership functions of angular velocity difference are defined as follows: 0°–50°, zero; 25°–75°, small; and 50°–100°, large. The membership functions of joint angle difference and angular velocity difference are depicted in Fig. 9. The fuzzy rule base for the rehabilitation is presented in Table 3.

To determine the joint ability, many joint angle calculations were conducted during every exercise. The following measurements were conducted during the chest press: eye level, left shoulder abduction, right shoulder abduction, left elbow flexion, and right elbow flexion. The following measurements were conducted during the seated row: left shoulder flexion, right shoulder flexion, left elbow flexion, and right elbow flexion. The following measurements were conducted during torso flexion: left shoulder flexion, right shoulder flexion, left elbow flexion, right elbow flexion, and right knee flexion. Finally, the following measurements were conducted during leg extension: eye level, left hip extension, right hip extension, left knee extension, and right knee extension. To display the functionalities of the wearable sensor devices, the proposed system considered right elbow joint movement for the chest press exercise as an example. Each participant was asked to wear a sensor-fitted jacket. Then, to determine whether the joint angles determined from the sensor data were within a reasonable measurement range from the beginning to the end of each rehabilitation movement, the postures of the participants were examined and set according to the rehabilitation exercise setting, as displayed in Fig. 10.

The participants wore detection devices on their upper or lower body according to the needs of different exercises and then performed the exercises in front of the webcam. Data were collected during the exercises to supplement the joint angle data. The Kalman filtering was used to extract important features and eliminate uncertainties (noises) from the recorded sensor data. Figures 11 and 12 present the raw sensor data and filtered signal for right elbow flexion, respectively.

From the collected data, the joint angle difference and angular velocity difference were calculated by comparing the sensor data with a benchmark set by a therapist according to the participants' joint movement ability. The blue, red, and yellow curves in Fig. 13a represent the actual joint angular velocity, the reference joint angular velocity, and the absolute difference between the actual and reference joint angular velocities, respectively. The blue, red, and yellow curves in Fig. 13b represent the actual joint angle, the reference joint angle, and the absolute difference between the actual and reference joint angles, respectively.

Table 1 Demographic data of the participants

Subjects	Age	Weight (kg)	Height (cm)	Gender
SA	24	50	178	Male
SB	25	64	165	Male
SC	23	72	178	Male
SD	24	72	168	Male
SE	22	71	172	Male
SF	23	73	174	Male
SG	23	60	160	Female
SH	25	65	170	Female
Mean ± SD	23.63 ± 1.06	65.88 ± 7.95	170.63 ± 6.25	

Table 2 Detailed descriptions of the joint exercises

Exercise	Feature description
Chest press	The body should be close to the back of the chair, and the arm should straighten to 0° when it is pushed. when it is lowered, the arm should be kept at 90° as far as possible, and the angle between the arm and the shoulder should be between 45° and 60°
Seated row	The body should be kept upright, with the angle between shoulder and arm between 0° and 15°, and the angle of arm bending between 90° and 120°
Torso flexion	When the body is bent, it should be 135° from the ground, the upper arm is 70° from the body, and the elbow joint is 0°. The head should not be too low or too high when bending, and the posture should be bilaterally symmetrical
Leg extension	When stretching the legs, start with the knee joint at 90°, and raise the saddle pads to make the knees straight. The angle of the knee joint can be greater than 90°, but not less than 90°

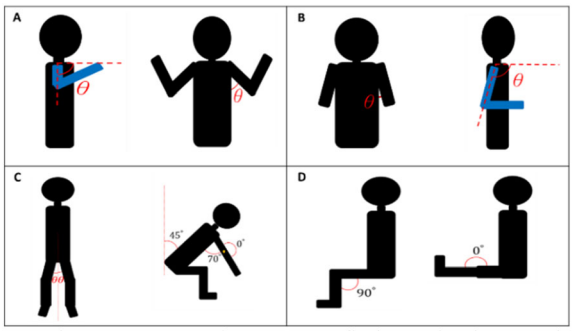

A. Chest press, B. seated row, C. torso flexion, and D. leg extension

Fig. 7 Postures of the conducted rehabilitation exercises

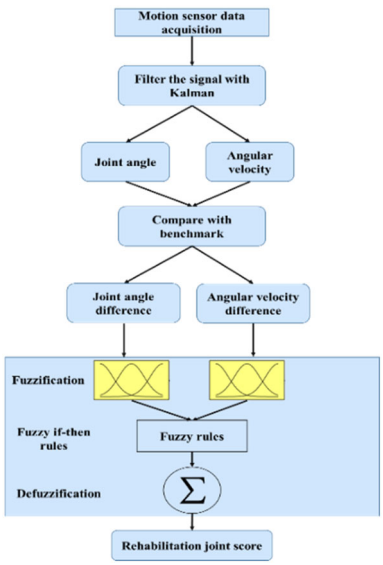

Fig. 8 FIS for the sensor data

Rehabilitation movements are mainly affected by the rhythm of exercise, which comprises a group of 10 eight-beat counts. To focus on ability recovery rehabilitation, we examined a 50-ms window before and after each extreme angle value at the beginning and end of each rehabilitation action. By fitting the angle difference and angular velocity difference into the proposed FIS to calculate the rhythm score, we obtained three to five scores for every 50-ms window of exercise. For every exercise, we encountered 20 window intervals for 20 extreme values. We obtained 69 window interval scores, as presented in Table 4.

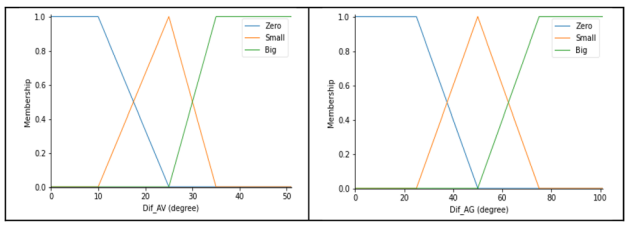

Fig. 9 Membership functions of the joint angle difference and angular velocity difference

Table 3 Fuzzy rule base

*Dif_AG	*Dif_AV		
	Zero	Small	Big
Zero	FS	HS	MS
Small	HS	MS	LS
Big	MS	LS	LS

**Dif_AG* difference angle, **Dif_AV* angular velocity difference, *LS* low score, *MS* medium score, *HS* high score, *FS* full score

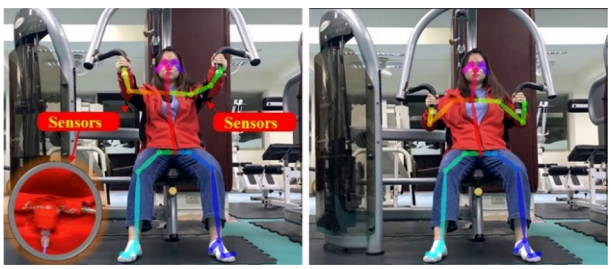

Fig. 10 Posture for the chest press exercise

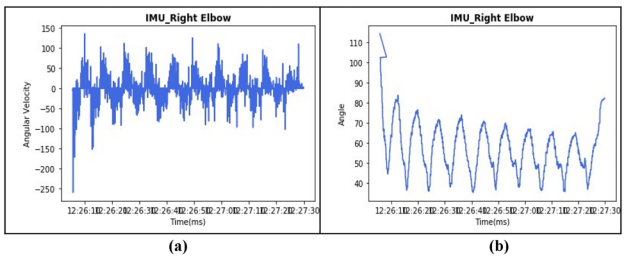

Fig. 11 Raw sensor data

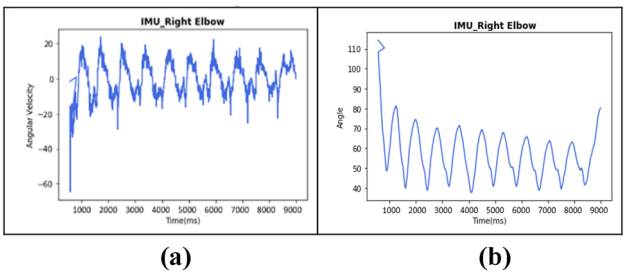

Fig. 12 Kalman-filtered signal data

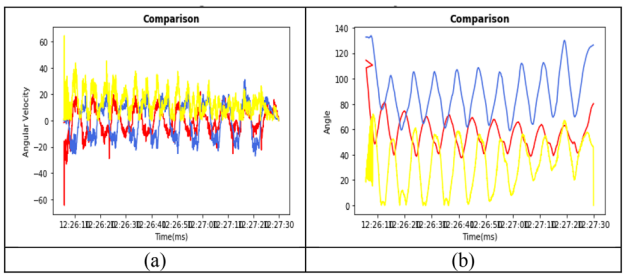

Fig. 13 Angular velocity and angle of the right elbow joint

The two highlighted scores in Table 4 represent the scores obtained in different intervals for right elbow flexion. For these scores, the output of the FIS is shown in Fig. 14. Figure 14a indicates that the score of 83.65 has an angle difference of 31.38 and an angular velocity difference of 8.51. Moreover, Fig. 14b indicates that the score of 90.01 has an angle difference of 24.45 and angular velocity difference of 11.83.

Finally, the average output for right elbow flexion was calculated from Table 4 (average score of 86.46).

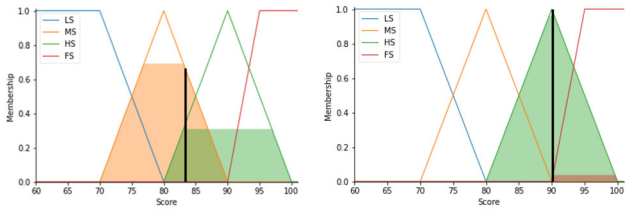

(a) Score of 83.65 for the right elbow

(b) Score of 90.01 for the right elbow

Fig. 14 FIS output score for right elbow flexion in the chest press exercise

Table 5 presents the scores obtained by participant SA in the different rehabilitation exercises (chest press, seated row, torso flexion, and leg extension). Based on his performance, leg extension scores for the left and right knees were slightly lower than his scores for other rehabilitation exercises. The scores obtained by participant SA indicate that he should take good care of his knee and focus more on knee rehabilitation. Moreover, from Fig. 15, we could predict the joint abilities of participant SA in a precise manner. For instance, the results obtained in the chest press indicated that the left shoulder abduction of participant SA was superior to his right shoulder abduction. Moreover, the left elbow flexion of participant SA was superior to his right elbow flexion. In the seated row and torso flexion exercises, the left shoulder flexion of participant SA was weaker than all the other joint movements. In the leg extension exercise, the left knee of participant SA exhibited higher extension than his right knee did. Thus, we could verify the joint movement ability using data collected during the different rehabilitation exercises.

Furthermore, to compare the joint actions and abilities of different individuals and groups, we used four rehabilitation machines. Initially, each machine was used to perform a rehabilitation action scoring test with two participants. After a participant completed their rehabilitation task on a machine, they performed further tasks on the other machines. The scores of participants SA and SB for the chest press conducted with the first rehabilitation machine are presented in Table 6. Participant SA marginally outperformed participant SB on left and right elbow flexion, whereas participant SB outperformed participant

Table 4 Participant SA's scores for right elbow flexion in the chest press exercise

80.37	80.42	80.69	80.68	92.27	92.28	92.28	92.14	92.51	92.43
92.42	92.51	92.51	92.27	92.28	92.29	92.29	92.27	86.58	87.03
91.87	85.77	85.39	85.35	84.91	86.11	86.55	86.56	86.91	81.76
81.91	81.74	81.93	81.93	82.07	92.16	92.06	92.05	91.88	81.26
81.40	81.40	81.53	92.45	92.43	92.43	92.46	83.08	83.28	83.28
83.65	90.01	90.00	90.01	81.98	82.03	81.84	81.85	85.04	84.90
84.86	84.63	82.37	82.46	80.20	80.20	82.34	82.45	82.32	
Average: 86.46									

Table 5 Scores obtained by participant SA in the four exercises

Chest press result				
Eye level	Left shoulder abduction	Right shoulder abduction	Left elbow flexion	Right elbow flexion
95.86	81.84	81.47	87.43	86.46
Seated row result				
Left shoulder flexion	Right shoulder flexion	Left elbow flexion	Right elbow flexion	
82.57	84.23	87.43	86.46	
Torso flexion result				
Left shoulder flexion	Right shoulder flexion	Left elbow flexion	Right elbow flexion	Right knee flexion
82.52	84.23	87.43	86.46	83.61
Leg extension result				
Eye level	Left hip extension	Right hip extension	Left knee extension	Right knee extension
94.63	85.32	86.23	80.74	80.53

SA on left and right shoulder abduction. The scores of participants SC and SD for the seated row exercise conducted with the second rehabilitation machine are presented in Table 7. In the aforementioned exercise, participant SC exhibited superior left and right shoulder flexion to participant SD, whereas participant SD exhibited superior left and right elbow flexion to participant SC. Table 8 presents the scores of participants SE and SF for the torso flexion exercise conducted with the third rehabilitation machine. In this exercise, participant SE exhibited superior performance to participant SF for all joint actions except right knee flexion. This result indicated that participant SE should be monitored for further exercise. Finally, the scores of participants SG and SH for the leg extension exercise conducted with the fourth rehabilitation machine are presented in Table 9. In this exercise, participant SG outperformed participant SH in left and right hip extension as well as right knee extension. The joint ability in other exercises can also be determined using the proposed system. The proposed system can provide qualitative and qualitative clinical rehabilitation suggestions by analyzing a person's joint movement ability during a set of rehabilitation exercises. Furthermore, the degrees of joint actions are computed to quantify the range of motion. Thus, effective rehabilitation management and accurate diagnosis can be achieved according to the severity of the injury and the disabling impairments faced by an individual.

5 Discussion

Physical activity and exercise are a vital determinant of functional capacity and health. Functional capacity and health have immediate and long-term importance in the prevention of disease and the improvement of the quality of life for people of all ages. Individuals may experience a decline in physical functions due to multiple health-related variables, such as progressive physical impairment caused by critical illness, injury, or surgery; the presence of medical disorders that limit mobility and muscle dysfunction; and age-related changes. Many elderly people experience a decline in physical functions as well as an increased prevalence of impairment and disability in their everyday life. Most frailty impairments lead to various medical issues, such as decreases in muscle mass strength, joint movement, cognitive ability, cardiorespiratory endurance, and postural control, as well as gait and musculoskeletal disorder. These problems are associated with mobility limitations, low gait speed, and a high risk of falls. Evidence indicated that compared with elderly people with high muscle strength, elderly people with low muscle strength are 2.6 times more susceptible to severe mobility limitations, are 4.3 times more susceptible to low gait speed, and have a 2.1 times higher mortality risk [23].

The loss of muscle strength and decline of balance (due to somatosensory issues) in elderly people cannot be explained only by the characteristic presence of skeletal muscle atrophy, neural sensory function, or the gravity center and supporting base physiology of these people. Therefore, the early recognition of physical impairment

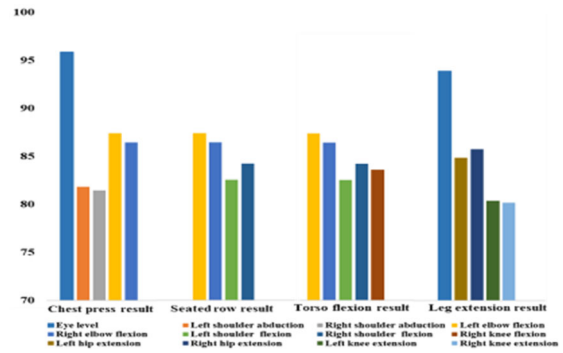

Fig. 15 Different exercises for joint movement rehabilitation

and correctly timed rehabilitation interventions are essential for addressing the needs of an aging society. In addition to the promotion of health, disease prevention, disease treatment, and palliative care, rehabilitation is an essential part of universal health coverage [24]. However, rehabilitation is generally conducted in hospitals by trained practitioners or other qualified health professionals. Rehabilitation facilities are not conveniently accessible to older patients, especially those living in isolated areas. Moreover, more than 50% of the people in some low- and middle-income countries are estimated to have insufficient access to the rehabilitation services they require. Existing rehabilitation services in 60–70% of countries worldwide have been disrupted due to the coronavirus disease 2019 pandemic [24]. Thus, in-home therapies have become a popular option for those most in need of rehabilitation services. Studies have used the Kinect device or motion sensor inertial measurement units (IMUs) with dynamic time warping (DTW) and fuzzy logic algorithms for the recognition of therapeutic movements and diagnosis of physical impairments. For instance, to assist patients in home-based rehabilitation, Su et al. [25] and Gal et al. [26] combined a Kinect-based system with the DTW algorithm and fuzzy logic to detect joint movements, postures, and motions in shoulder rehabilitation for physical impairments. Furthermore, to assist patients with knee osteoarthritis in self-rehabilitation at home, Chen et al. [27] used three wearable sensors (i.e., triaxial accelerometers) that were mounted on the chest, thigh, and shank of the working leg. The system of Chen et al. used the collected angle information as well as the time- and frequency-domain features of sensor signals to identify the type of rehabilitation exercise. Moreover, hierarchical methods were implemented to detect improper exercise movements of the patient. Rybarczyk et al. [28] introduced a web-based platform to conduct physical telerehabilitation for patients who had undergone hip arthroplasty surgery. A Kinect camera was used to capture the hip abduction and trunk movements of the patient. The camera was connected to the Django website to manage the data flow of the patients. To develop an intelligent environment for con-

Table 6 Chest press results for participants SA and SB

Chest press	Eye level	Left shoulder abduction	Right shoulder abduction	Left elbow flexion	Right elbow flexion
SA	95.86	81.84	81.47	87.43	86.46
SB	94.63	82.93	81.65	86.92	85.32

Table 7 Seated row results for participants SC and SD

Seated row	Left shoulder flexion	Right shoulder flexion	Left elbow flexion	Right elbow flexion
SC	81.57	86.62	79.40	85.14
SD	78.66	84.71	82.55	86.57

Table 8 Torso flexion result for participants SE and SF

Torso flexion	Left shoulder flexion	Right shoulder flexion	Left elbow flexion	Right elbow flexion	Right knee flexion
SE	79.16	81.34	84.77	84.38	87.91
SF	80.51	82.62	85.14	84.96	86.85

Table 9 Leg extension result for participants SG and SH

Leg extension	Eye level	Left hip extension	Right hip extension	Left knee extension	Right knee extension
SG	91.52	88.23	88.91	83.51	83.61
SH	90.20	86.52	86.57	84.74	82.58

Table 10 Comparison of the proposed system with different existing rehabilitation systems

Existing approaches	Algorithm	Devices	Rehabilitation	GUI interface	Additional features	Rehabilitation settings	Application
Su et al. [25]	DTW, FL	Kinect	Shoulder rehabilitation	Presented	No	Home	Joints movement
Gal et al. [26]	DTW, FL	Kinect	Physical impairments	Presented	No	Home	Posture and motion range
Chen et al. [27]	MF, FFT, BC, KNN	AG	knee osteoarthritis rehabilitation	No	Error alarm	Home	Knee joint movement
Rybarczyk et al. [28]	HMMs, Django	Kinect	Hip arthroplasty surgery	Presented	Identify the motion errors	Home	Hip abduction and trunk movement
Oliver et al. [29]	FIS	VTD	Cognitive rehabilitation	Presented	No	Home	Cognitive
Bell et al. [30]	SMAA, KF	IMU, MA	Knee rehabilitation	Presented with visual feedback	No	Home	Knee joint movement
Chen et al. [31]	ICC, MWUT	IMU, MA	Adhesive capsulitis (AC) of the shoulder	Avatar presented	No	Home	Shoulder
Our	DCM, KF, FIS, OP	IMU, MA	Power rehabilitation, general rehabilitation and elderly with Parkinson disease	Avatar presented, alert with wrong joint movements	Individual guide video is played for the reference exercise for each participant Audio instruction is provided Overcome joint movements occlusion	Home and hospital	Joints movement, range of motion, and posture

DTW dynamic time warping, *FL* fuzzy logic, *MF* median filter, *FFT* fast Fourier transform, *BC* Bayesian classifier, *KNN* k-nearest neighbors, *HMMs* hidden Markov models, *FIS* fuzzy inference system, *SMAA* static manual anatomical alignment, *KF* Kalman filter, *ICC* intraclass correlation coefficient, *MWUT* Mann–Whitney *U* test, *DCM* direction cosine matrix, *OP* OpenPose, *AG* accelerometer and gyroscope, *VTD* VIbroTActile toolkit device, *IMU* inertial measurement unit, *MA* mobile app

ducting cognitive rehabilitation at home, Oliver et al. [29] used an FIS with the VIbroTActile toolkit device to collect expertise from a rehabilitation expert. Knee injury or surgery is critical for the recovery of function and independence. Bell et al. [30] used IMU motion tracking sensors and an OptiTrack system to detect the joint angle of knee motion during rehabilitation exercises. Chen et al. [31] developed a home-based shoulder rehabilitation system that comprised an IMU and a mobile app for patients and physicians to trace and monitor shoulder mobility measurements. However, unlike other studies that focused only on certain types of rehabilitation, such as shoulder, knee, hip, and cognitive rehabilitation, the present study developed a comprehensive approach for conducting and examining various types of rehabilitation. To verify the

feasibility of the proposed system, its features were compared with those of existing systems (Table 10).

Rehabilitation actions help disabled people to regain their movement ability; however, during closed-chain rehabilitation exercises and rehabilitation exercises with different posture orientations, the Kinect device may be unable to overcome the issue caused by the occlusion of joints and postures. Moreover, the calibration of repetitive movement may be inaccurate for identifying human skeletal features. Thus, evaluating certain types of rehabilitation exercises with the Kinect device is difficult. To overcome the issues caused by the poor occlusion of joints and postures, we integrated a self-designed IMU and OpenPose to capture every joint segment and human skeleton node. Furthermore, an FIS-based evaluation system was developed to describe the values of attributes as degrees of likelihood and address the vagueness and uncertainties of joints movements. The joint inputs are transformed into degrees of membership by projecting the input numerical values into a set of membership functions using fuzzy set inference. The degree of membership acquired is a fuzzy representation of the extent to which the linguistic value is satisfied and is used as a factor for decision-making based on fuzzy rules of joint movement ability.

The proposed system can be implemented in various types of rehabilitation trials, such as power rehabilitation, general rehabilitation, and rehabilitation for elderly people with PD. The system conducts multicriteria decision-making on the basis of joint movements and range of motion, as presented in Fig. 15 and Tables 6, 7, 8 and 9. Each patient's joint movement ability is different, and exercise recordings for one patient may not be suitable for use by others even if they have the same disability of joint movements. The proposed system can provide comprehensive and individual guidance according to each user's need.

The sensors connected to patients are virtually simulated by a virtual-reality avatar, which precisely identifies and indicates incorrect joint movements. Thus, the proposed system provides an attractive virtual environment for assessing the quality of rehabilitation movements in both in-home and hospital settings.

6 Conclusions

In this study, we developed a system comprising a web camera and IMUs that can capture angles of the human posture and joints. An FIS was used to score patient rehabilitation actions and prompt suggestions for joint movement ability. The interactive interface overcomes the problem of patients forgetting a rehabilitation movement by reminding them intuitively to correct their posture and joint angles to improve the quality of rehabilitation. The proposed system not only allows physicians to access quantitative reference data for improving rehabilitation quality but also helps patients with PD to notice blind spots and the occlusion of the joint angle using an inertial sensing unit, without which they may ignore such spots and occlusion during rehabilitation. Patients can follow the standard rehabilitation videos provided by the proposed system to perform rehabilitation exercises even at home, and they can track their progress without the presence of a medical practitioner.

In this study, joint angle simulation was performed for students. In the future, we will include elderly individuals to obtain more practical results.

Acknowledgements This study was funded in part by the Ministry of Science and Technology, Taiwan, under Grant MOST108-2221-E-027-111-MY3 and in part by the joint project between the National Taipei University of Technology and the Chang Gung Memorial Hospital under Grants NTUT-CGMH-106-05 and NTUT-CGMH-109-01.

References

1. UN: Peace, Dignity and Equality on a Healthy Planet. https://www.un.org/en/sections/issues-depth/ageing/. Accessed 22 June 2020
2. Morley, J.E., Arai, H., Cao, L., et al.: Integrated care: enhancing the role of the primary health care professional in preventing functional decline: a systematic review. J. Am. Med. Dir. Assoc. **18**(6), 489–494 (2017)
3. Abete, P., Basile, C., Bulli, G., et al.: The Italian version of the "Frailty Index" based on deficits in health: a validation study. Aging Clin. Exp. Res. **29**(5), 913–926 (2017)
4. Fong, T.G., Tulebaev, S.R., Inouye, S.K.: Delirium in elderly adults: diagnosis, prevention and treatment. Nat. Rev. Neurol. **5**(4), 210–220 (2009)
5. Shimada, H., Makizako, H., Lee, S., et al.: Impact of cognitive frailty on daily activities in older persons. J. Nutr. Health Aging **20**(7), 729–735 (2016)
6. Liguori, I., Russo, G., Aran, L.: Sarcopenia: assessment of disease burden and strategies to improve outcomes. Clin. Interv. Aging **13**, 913–927 (2018)
7. Cheung, J.T.K., Yu, R., Wu, Z., et al.: Geriatric syndromes, multimorbidity, and disability overlap and increase healthcare use among older Chinese. BMC Geriatr. **18**, 1–8 (2018)
8. Sanford, A.M., Morley, J.E., Berg-Weger, M., et al.: High prevalence of geriatric syndromes in older adults. PLoS ONE **15**(6), 1–8 (2020)
9. Staszewski, J., Piusińska-Macoch, R., Brodacki, B., et al.: Vascular Parkinsonism and vascular dementia are associated with an increased risk of vascular events or death. Arch. Med. Sci. Atheroscler. Dis. **2**(1), e16–e23 (2017)
10. Young, C., Edwards, C., Singh, I.: Impact of hospital design on acutely unwell patients with dementia. Geriatrics **2**(1), 1–9 (2017)
11. Reynish, E.L., Hapca, S.M., De Souza, N., et al.: Epidemiology and outcomes of people with dementia, delirium, and unspecified cognitive impairment in the general hospital: prospective cohort study of 10,014 admissions. BMC Med. **15**(1), 1–12 (2017)

12. Holstege, M.S., Caljouw, M.A.A., Zekveld, I.G., et al.: Successful geriatric rehabilitation: effects on patients' outcome of a national program to improve quality of care, the SINGER Study. J. Am. Med. Dir. Assoc. **18**(5), 383–387 (2017)
13. Cai, L., Ma, Y., Xiong, S., Zhang, Y.: Validity and reliability of upper limb functional assessment using the Microsoft Kinect V2 sensor. Appl. Bionics Biomech. **2019**, 1–14 (2019)
14. Singh, I., Fernando, P., Griffin, J.: Clinical outcome and predictors of adverse events of an enhanced older adult psychiatric liaison service: rapid assessment interface and discharge (Newport). Clin. Interv. Aging **12**, 29–36 (2016)
15. Stucki, G., Bickenbach, J., Gutenbrunner, C., Melvin, J.: Rehabilitation: the health strategy of the 21st century. J. Rehabil. Med. **50**(4), 309–316 (2018)
16. Kan, Y.C., Kuo, Y.C., Lin, H.C.: Personalized rehabilitation recognition for ubiquitous healthcare measurements. Sensors **19**(7), 1–23 (2019)
17. Duprey, S., Naaim, A., Moissenet, F., Begon, M., Cheze, L.: Kinematic models of the upper limb joints for multibody kinematics optimisation: an overview. J. Biomech. **62**, 87–94 (2017)
18. Jackson, M., Michaud, B., Tetreault, P., Begona, M.: Improvements in measuring shoulder joint kinematics. J. Biomech. **45**(12), 2180–2218 (2012)
19. Díaz-Curbelo, A., Espin Andrade, R.A., Gento Municio, Á.M.: The role of fuzzy logic to dealing with epistemic uncertainty in supply chain risk assessment: review standpoints. Int. J. Fuzzy Syst. (2020). https://doi.org/10.1007/s40815-020-00846-5
20. Dourado, A.D., Lobato, F.S., Cavalini, A.A., et al.: Fuzzy reliability-based optimization for engineering system design. Int. J. Fuzzy Syst. **21**, 1418–1429 (2019)
21. Amirkhani, A., Nasiriyan-Rad, H., Papageorgiou, E.I.: A novel fuzzy inference approach: neuro-fuzzy cognitive map. Int. J. Fuzzy Syst. **22**, 859–872 (2020)
22. Cao, Z., Hidalgo, G., Simon, T., Wei, S.-E., Sheikh, Y.: OpenPose: Realtime Multi-person 2D Pose Estimation Using Part Affinity Fields. arXiv preprint (2018). arXiv:1812.08008
23. Manini, T.: Development of physical disability in older adults. Curr. Aging Sci. **4**(3), 184–191 (2011)
24. WHO: Rehabilitation. https://www.who.int/news-room/fact-sheets/detail/rehabilitation. Accessed 5 July 2020
25. Su, C.-J., Chiang, C.-Y., Huang, J.-Y.: Kinect-enabled home-based rehabilitation system using dynamic time warping and fuzzy logic. Soft Comput. **22**, 652–666 (2014)
26. Gal, N., Andrei, D., Nemeş, D.I., Nădăşan, E., Stoicu-Tivadar, V.: A Kinect based intelligent e-rehabilitation system in physical therapy. Stud. Health Technol. Inform. **210**, 489–493 (2015)
27. Chen, K.-H., Chen, P.-C., Liu, K.-C., Chan, C.-T.: Wearable sensor-based rehabilitation exercise assessment for knee osteoarthritis. Sensors **15**(2), 4193–4211 (2015)
28. Rybarczyk, Y., Kleine, D.J., Cointe, C., Esparza, D.: Smart web-based platform to support physical rehabilitation. Sensors (Basel) **18**(5), 1–21 (2018)
29. Oliver, M., Teruel, M.A., Molina, J.P., Romero-Ayuso, D., González, P.: Ambient intelligence environment for home cognitive telerehabilitation. Sensors (Basel) **18**(11), 1–30 (2018)
30. Bell, K.M., Onyeukwu, C., McClincy, M.P., et al.: Verification of a portable motion tracking system for remote management of physical rehabilitation of the knee. Sensors (Basel) **19**(5), 1–13 (2019)
31. Chen, Y.P., Lin, C.Y., Tsai, M.J., Chuang, T.Y., Lee, O.K.: Wearable motion sensor device to facilitate rehabilitation in patients with shoulder adhesive capsulitis: pilot study to assess feasibility. J. Med. Internet Res. **22**(7), e17032 (2020)

Yo-Ping Huang received the Ph.D. Degree in Electrical Engineering from Texas Tech University, Lubbock, TX, USA. He is currently a Chair Professor in the Department of Electrical Engineering, National Taipei University of Technology, Taipei, Taiwan, where he served as the Secretary General. He was a Professor and the Dean of Research and Development, the Dean of the College of Electrical Engineering and Computer Science, and the Department Chair with Tatung University, Taipei. His current research interests include fuzzy systems design and modeling, deep learning modeling, intelligent control, medical data mining, and rehabilitation systems design. Professor Huang serves as the IEEE SMCS BoG, Chair of the IEEE SMCS Technical Committee on Intelligent Transportation Systems, and the Chair of the Taiwan SIGSPATIAL ACM Chapter. He was the President of the Taiwan Association of Systems Science and Engineering, the Chair of IEEE SMCS Taipei Chapter, the Chair of the IEEE CIS Taipei Chapter, and the CEO of the Joint Commission of Technological and Vocational College Admission Committee, Taiwan. He is an IEEE Fellow, IET Fellow, CACS Fellow, and an International Association of Grey System and Uncertain Analysis Fellow.

Wen-Lin Kuo is a Ph.D. Student in the Department of Electrical Engineering, National Taipei University of Technology, Taipei, Taiwan. Her research work focuses on the elderly care, fitness applications, image processing and data analysis.

Haobijam Basanta received Master of Science in Computer Application (MCA) from the University of Jamia Millia Islamia, Delhi, India. He received his Ph.D. Degree in Electrical Engineering and Computer Science at National Taipei University of Technology, Taipei, Taiwan. He is currently a Post Doctor at the same institution. His current research interests include Artificial Intelligence (AI), Internet of Things (IoT) for elderly healthcare system, big data analytics, deep learning and image processing.

Si-Huei Lee received the Ph.D. Degree in Department of Health and Welfare, Niigata University of Health and Welfare, Japan. She is currently a Rehabilitation Physician in the Veterans General Hospital, Taipei, Taiwan. She is an Assistant Professor in the Department of Medicine, National Yangming Chiaotung University, Taipei, Taiwan. Her current research interests include smart rehabilitation, medical data mining, and rehabilitation systems design.